Temperature dependence of the fractional thermal load of Nd:YVO_4 at 1064 nm lasing and its influence on laser performance

Yajun Wang, Wenhai Yang, Haijun Zhou, Meiru Huo, Yaohui Zhen*

State Key Laboratory of Quantum Optics and Quantum Optics Devices, Institute of Opto-Electronics, Shanxi University, Taiyuan 030006, China

*yhzheng@sxu.edu.cn

Abstract: Temperature dependence of thermal effect for neodymium doped yttrium orthovanadate crystal is quantified by measuring its dioptric power. With the boundary temperature range from 293 K to 353 K, the increase of fractional thermal load (lasing at 1064 nm, pumping at 888 nm) is from 16.9% to 24.9% with lasing, which is attributed to the rise of upconversion parameter and thermal conductivity. The influence of the boundary temperature on the output characteristic of a high-power single frequency laser is also investigated. The maximum output power decreases from 25.3 W to 13.5 W with the increase of boundary temperature from 293 K to 353 K. Analysis results indicate that further power scaling can be achieved by controlling the Nd:YVO_4 temperature to a lower.

OCIS codes: (140.3460) Lasers; (140.3480) Lasers, diode-pumped; (140.3613) Lasers, upconversion; (140.6810) Thermal effects; (140.3515) Lasers, frequency doubled; (140.3530) Lasers, laser neodymium.

References and links

1. Y. F. Chen, and Y. P. Lan, "Comparison between c-cut and α-cut Nd:YVO_4 lasers passively Q-switched with a Cr^{4+}:YAG saturable absorber," Appl. Phys. B **74**(4-5), 415-418 (2002).
2. W. Koechner, "Thermo-Optic Effects and Heat Removal," in *Solid-State Laser Engineering*, W. T. Atlanta, eds. (Academic, New York, 1999), pp.406-407.
3. P. Dekker, H. M. Pask, D. J. Spence, and J. A. Piper, "Continuous-wave, intracavity doubled, self-Raman laser operation in Nd:$GdVO_4$ at 586.5 nm," Opt. Express **15**(11), 7038-7046 (2007).
4. S. R. Bowman, S. P. Oconnor, S. Biswal, N. J. Condon, and A. Rosenberg, "Minimizing heat generation in solid-state lasers," IEEE J. Quantum Electron. **46**(7),1076-1085 (2010).
5. F. Lenhardt, M. Nittmann, T. Bauer, J. Bartschke, and J. A. Lhuillier, "High-power 888-nm-pumped Nd:YVO_4 1342-nm oscillator operating in the TEM_{00} mode," Appl. Phys. B **96**(4), 803-807 (2009).
6. C. Jacinto, S. L. Oliveira, T. Catunda, A. A. Andrade, J. D. Myers, and M. J. Myers, "Upconversion effect on fluorescence quantum efficiency and heat generation in Nd^{3+}-doped materials," Opt. Express **25**(6), 2040-2046 (2005).
7. J. D. Zuegel, and W. Seka, "Upconversion and reduced $^4F_{3/2}$ upper-state lifetime in intensely pumped Nd:YLF," Appl. Opt. **38**(12), 2714-2723 (2002).
8. C. Jacinto, D. N. Messias, A. A. Andrade, and T. Catunda, "Energy transfer upconversion determination by thermal-lens and Z-scan techniques in Nd^{3+}-doped laser materials," J. Opt. Soc. Am. B **26**(5), 1002-1007 (2009).
9. A. Camargo, C. Jacinto, T. Catunda, and L. Nunes, "Auger upconversion energy transfer losses and efficient 1.06 μm laser emission in Nd^{3+} doped fluoroindogallate glass," Appl. Phys. B **83**(4), 565-569 (2006).
10. J. L. Blows, T. Omatsu, J. Dawes, H. Pask, and M. Tateda, "Heat generation in Nd:YVO_4 with and without laser action," IEEE Photon. Technol. Lett. **10**(12), 1727-1729 (1998).

#191256 - $15.00 USD Received 28 May 2013; revised 12 Jul 2013; accepted 12 Jul 2013; published 19 Jul 2013

11. X. Delen, F. Balembois, O. Musset, and P. Georges, "Characteristics of laser operation at 1064 nm in Nd:YVO_4 under diode pumping at 808 and 914 nm," J. Opt. Soc. Am. B **28**(1), 52-57 (2011).
12. L. Meilhac, G. Pauliat, and G. Roosen, "Determination of the energy diffusion and the auger upconversion constants in a Nd:YVO_4 standing wave laser," Opt. Commun **203**(3-7), 341-347 (2002).
13. Y. F. Chen, C. C. Liao, Y. P. Lan, and S. C. Wang, "Determination of the auger upconversion rate in fiber-coupled diode end-pumped Nd:YAG and Nd:YVO_4 crystals," Appl. Phys. B **70**(4), 487-490 (2000).
14. T. Chuang, and H. R. Verdun, "Energy transfer up-conversion and excited state absorption of laser radiation in Nd:YLF laser crystals," IEEE J. Quantum Electron. **32**(1), 79-91 (1996).
15. C. Jacinto, T. Catunda, D. Jaque, L. E. Bausa, and J. G. Sole, "Thermal lens and heat generation of Nd:YAG lasers operating at 1.064 and 1.34 μm," Opt. Express **16**(9), 6317-6323 (2008).
16. I. O. Musgrave, "Study of the physics of the power-scaling of end-pumped solid-state laser sources based on Nd:YVO_4," Doctor Thesis, pp. 50-54.
17. X. Delen, F. Balembois, and P. Georges, "Temperature dependence of the emission cross section of Nd:YVO_4 around 1064 nm and consequences on laser operation," J. Opt. Soc. Am. B **28**(5), 972-976 (2011).
18. G. Turri, H. P. Jenssen, F. Cornacchia, M. Tonelli, and M. Bass, "Temperature-dependent stimulated emission cross section in Nd:YVO_4 crystals," J. Opt. Soc. Am. B **26**(11), 2084-2088 (2009).
19. A. Rapaport, S. Zhao, G. Xiao, A. Howard, and M. Bass, "Temperature dependence of the 1.06-μm stimulated emission cross section of neodymium in YAG and in GSGG," Appl. Opt. **41**(33), 7052-7057 (2002).
20. R. Kapoor, P. K. Mukhopadhyay, J. George, and S. K. Sharma, "Thermal lens measurement technique in end-pumped solid state lasers: Application to diode-pumped microchip lasers," Pramana-J. Phys. **52**(6), 623-629 (1999).
21. P. J. Hardman, W. A. Clarkson, G. J. Friel, M. Pollnau, and D. C. Hanna, "Energy-transfer upconversion and thermal lensing in high-power end-pumped Nd:YLF laser crystals," IEEE J. Quantum Electron. **35**(4), 647-655 (1999).
22. M. E. Innocenzi, H. T. Yura, C. L. Fincher, and R. A. Fields, "Thermal modeling of continuous-wave end-pumped solid-state lasers," Appl. Phys. Lett. **56**(19), 1831-1833 (1990).
23. J. C. Bermudez, V. J. Pinto-Robledo, A. V. Kiryanov, and M. J. Damzen, "The thermo-lensing effect in a grazing incidence, diode-side-pumped Nd:YVO_4 laser," Opt. Commun. **210**(9), 75-82 (2002).
24. D. E. Zelmon, J. J. Lee, K. M. Currin, J. M. Northridge, and D. Perlov, "Revisiting the optical properties of Nd doped yttrium orthovanadate," Appl. Opt. **49**(4), 644-647 (2010).
25. Y. F. Chen, T. M. Huang, C. F. Kao, C. L. Wang, and S. C. Wang, "Optimization in scaling fiber-coupled laser-diode end-pumped lasers to higher power: Influence of thermal effect," IEEE J. Quantum Electron. **33**(8), 1424-1429 (1997).
26. J. K. Jabczynski, "Modeling of diode pumped laser with pump dependent diffraction loss," Opt. Commun. **182**(4-6), 413-422 (2000).
27. W. A. Clarkson, "Thermal effects and their mitigation in end-pumped solid-state lasers," J. Phys. D: Appl. Phys. **34**(16), 2381-2395 (2001).
28. Y. J. Wang, Y. H. Zheng, C. D. Xie, and K. C. Peng, "High-power, low-noise Nd:YAP/LBO laser with dual wavelength outputs," IEEE J. Quantum Electron. **47**(7), 1006-1013 (2011).
29. Y. H. Zheng, Y. J. Wang, C. D. Xie, and K. C. Peng, "Single-frequency Nd:YVO_4 laser at 671 nm with high-output power of 2.8 W," IEEE J. Quantum Electron. **48**(1), 67-71 (2012).
30. M. O. Ramirez, D. Jaque, L. E. Bausa, I. R. Martin, F. Lahoz, E. Cavalli, A. Speghini, and M. Bettinelli, "Temperature dependence of $Nd^{3+} \longleftrightarrow Yb^{3+}$ energy transfer in the $YAl_3(BO_3)_4$ nonlinear laser crystal," J. Appl. Phys. **97**(9), 093510 (2005).
31. S. D. Xia, and P. A. Tanner, "Theory of one-phonon-assisted energy transfer between rare-earth ions in crystals," Phys. Rev. B **66**(21), 214305 (2002).
32. D. K. Sardar, and R. M. Yow, "Stack components of $^4F_{3/2}$, $^4I_{9/2}$ and $^4I_{11/2}$ manifold energy levels and effects of temperature on the laser transition of Nd^{3+} in YVO_4," Opt. Mater. **14**(1), 5-11 (2000).
33. W. M. Yen, W. C. Scott, and A. L. Schawlow, "Phonon-induced relaxation in excited optical states of trivalent praseodymium in LaF_3," Phys. Rev. **136**(1A), A271-A283 (1964).
34. H. Kogelnik, and T. Li, "Laser beams and resonators," Appl. Opt. **5**(10), 1550-1566 (1966).
35. Y. H. Zheng, F. Q. Li, Y. J. Wang, K. S. Zhang, and K. C. Peng, "High-stability single-frequency green laser with a wedge Nd:YVO_4 as a polarizing beam splitter," Opt. Commun. **283**(2), 309-312 (2010).

1. Introduction

The Nd:YVO_4 (Neodymium doped yttrium orthvanadate) transitions at 1064 nm have been widely used for laser applications, because it offers several advantages over other laser systems: its large stimulated-emission cross section at 1064 nm and high absorption over a wide pumping wavelength bandwidth allow a low laser threshold and a high slope efficiency. YVO_4

#191256 - $15.00 USD Received 28 May 2013; revised 12 Jul 2013; accepted 12 Jul 2013; published 19 Jul 2013

crystal is naturally birefringent and laser output is linearly polarized, which avoids undesirable depolarization loss [1]. The transition of $^4F_{3/2}$-$^4I_{11/2}$ is a four-level process with fast multi-phonon transitions populating the upper and depleting the lower laser level. Due to the energy difference between the pump and the laser photons, the optical pumping process is associated with the generation of heat. The thermal effect has a number of undesirable consequences, such as spherical aberration with consequent degradation in laser beam quality and resonator losses. Ultimately, rod fracture will occur [2]. Additionally, the thermal lens (TL) resulting from the thermal effect is a critical factor for optimizing resonator design and scaling the output power of the laser [3]. So mitigating and quantifying the thermal effect have been the focus of the study of high-power lasers [4, 5].

In-band pumping is one of the best methods of reducing the quantum defect heating. However, due to the influence of energy transfer upconversion (ETU) and excited-state absorption (ESA), the quantum defect is not the only factor of determining the thermal effect [5-9]. Some papers have mentioned a significant impact of doping concentration and laser regime (lasing or nonlasing) on the thermal effect of the Nd:YVO_4 crystal [10-13]. Comparing with lasing, the Nd:YVO_4 laser system exhibits a significantly increasing thermal effect under conditions of nonlasing [10, 14]. This behavior has been explained by probability increase of ETU owing to higher population density in the upper lasing level [10, 15]. The phenomenon that the thermal effect arises with the increase of doping concentration attributes to smaller ion spacing in higher doping crystals, which increase the probability of ETU [16]. The ETU processes cause extra heat to be generated in the Nd:YVO_4 crystal, exacerbating thermal problems caused by the conversion of pump power into heat.

Recently, some authors did also mention a significant impact of temperature on Nd:YVO_4 emission wavelength, emission cross section, and line width, at the emission wavelength around 1064 nm [17-19]. However, until now, the influence of absolute boundary temperature of Nd:YVO_4 crystal on the thermal effect and the output power of high-power laser has not been studied.

In this paper, the influence of the boundary temperature of Nd:YVO_4 on the thermal effect (related to the fractional thermal load induced from quantum effect and ETU) and laser performance is investigated in detail. In order to quantify the thermal effect, we measure the dioptric power of the Nd:YVO_4 crystal at different boundary temperatures with lasing. Based on the measuring results, we simulate the fractional thermal load and the upconversion parameter at different boundary temperatures. With lasing, the upconversion parameter increases with the rise of the boundary temperature. The input-output relationship over the usual laser operation temperature range is shown, respectively. The results show that the thermal effect intensifies, the maximum output power and conversion efficiency decreases, with the rise of boundary temperature.

2. Theoretical background

During the optical pumping process, a fraction of absorbed pump power is converted into heat, generating a radial temperature gradient. The temperature gradient results in refractive index gradient and stress-dependent refractive gradient along the radial directions of the laser medium, and consequently, creating a lens-like element in the crystal. The focal length of the TL is in inverse proportion to its dioptric power, which is a critical factor for laser design. In order to make the measuring results of the TL correspond to the actual laser setup, the TL is indirectly calculated by measuring the parameter of the output beam (the waist size or divergence angle) of the Nd:YVO_4 single frequency laser system. The parameter of the output beam is measured via a M^2 meter (DataRay. Inc).

The single-frequency laser cavity can be described in terms of an infinite wave-guide of

#191256 - $15.00 USD Received 28 May 2013; revised 12 Jul 2013; accepted 12 Jul 2013; published 19 Jul 2013

repeated optical components. The optical path for one round trip inside the resonator can be expressed by ABCD transfer matrix, which is obtained from the individual ABCD matrices of the resonator components. In view of the astigmatism of off-axis concave mirrors in the ring cavity, we build the ABCD transfer matrix in the sagittal plane or the tangential plane, and then measure the characteristic of the output beam (the waist size and divergence angle) in the corresponding plane via a M^2 meter. In these optical components, except for the focal length of the TL, all other optical components are known. Once the characteristic of the output beam (the waist size and divergence angle) is measured, it is very easy to deduce the focal length of the TL (that is dioptric power) of the gain medium [20]. The accuracy of this technique is limited by the uncertainty in the measurement of the cavity length, the incident angle of the concave mirrors, and the output beam parameter. The combined of these uncertainties results in systematic error for the dioptric power within the range $\pm$30% [21].

In addition, the dioptric power, D, can be given by [22]:

$$D = \frac{\eta_h P_{abs}}{\pi K \omega_p^2} \frac{ds}{dT}. \tag{1}$$

in which P_{abs} is the absorption pump power, which can be expressed by $P\times[1\text{-}exp(\text{-}\alpha l)]$, P is the pump power, α is the absorption coefficient, l is the length of the Nd:YVO_4, η_h is the fractional thermal load, K is the thermal conductivity, ω_p is the pump beam radius, and ds/dT is the combined effects of the temperature-dependent (dn/dT) and stress-dependent variation of the refractive index of the gain medium. The temperature-dependent variation of the refractive index constitutes the major contribution of the dioptric power, whilst the stress-dependent variation of the refractive index has a minor contribution. The percentage weight of the combined effects of the stress term is less than 3.7%, so we neglect the influence of stress-dependent variation of the refractive index on the dioptric power in the analysis process [23].

The pump beam radius ω_p is constant for the specific experiment. Both the thermal conductivity K and the thermo-optical coefficient dn/dT are related to the temperature of the Nd:YVO_4 . The variation of the boundary temperature does also result in an opposite change in thermal conductivity K and a positive change in thermo-optical coefficient dn/dT. The temperature dependence of thermal conductivity K is approximately given by

$$K(T) = K_0 \frac{T_0}{T} \tag{2}$$

Where T is the absolute temperature and K_0 is the thermal conductivity at a characteristic temperature T_0. For Nd:YVO_4, K_0 =5.23 W/m·K at T_0=300 K. Based on the Eq. (2), the thermal conductivity K at different boundary temperature can be calculated. The temperature dependence of thermo-optical coefficient dn/dT is approximately expressed by [24]

$$\frac{dn(T)}{dT} = A - B(T - 296) \tag{3}$$

Where A and B are constant. However, B is only less than 10^{-4} of A (the uncertainty of the dn/dT is only 0.1% or so in the temperature range of our measurement), the dependence of the dn/dT on the temperature can be neglected.

Generally, the fractional thermal load η_h is only related to quantum defect η_q (defined by $(\lambda_l\text{-}\lambda_p)/\lambda_l$, where λ_l is the laser wavelength and λ_p is the pump wavelength). However, due to high population inversion in high power laser, ETU process must be considered, accompanied by additional heat sources, then the fractional thermal load can be higher than the one brought by only quantum defect. If we consider the influence of ETU process on the fractional thermal

#191256 - $15.00 USD Received 28 May 2013; revised 12 Jul 2013; accepted 12 Jul 2013; published 19 Jul 2013

load, η_h can be expressed as [11]:

$$\eta_h = \eta_q + \frac{\lambda_p}{R\lambda_l}(\frac{\Delta n}{\tau_{nr}} + \gamma \Delta n^2). \tag{4}$$

where η_q is the thermal load induced from quantum defect, R is the pumping rate and is given by $R=P_{abs}/h\nu_p V$, γ is the upconversion parameter, $h\nu_p$ is the pump photon energy, V is the volume of pumping region in Nd:YVO_4, τ_{nr} is nonradiative decay time, Δn is the population inversion density. For the sake of simplicity, the nonradiative decay τ_{nr} are supposed to be constant at different boundary temperatures, and the population inversion density Δn does only have relation to the losses of the laser, independent of the absorbed pump power, above threshold.

Considering the ETU effect, the expression for the dioptric power D becomes:

$$D = CK^{-1}\eta_h P_{abs}. \tag{5}$$

where $C=(\pi\omega_p^2)^{-1}ds/dT$. For the positive experiment system, C is a constant. Substituting (4) into (5), the dioptric power D can be found to be

$$D = CK^{-1}\eta_q P_{abs} + CK^{-1}h\nu_l V(\frac{\Delta n}{\tau_{nr}} + \gamma \Delta n^2). \tag{6}$$

It can be found, from Eq. (6), that the dioptric power D is theoretically linear with the absorption pump power P_{abs} at a certain boundary temperature. $CK^{-1}\eta_q$ stands for the slope of the line, $CK^{-1}h\nu_l V(\Delta n/\tau_{nr} + \gamma\Delta n^2)$ stands for the intercept of the line. Based on Eq. (6) and the measuring results of the dioptric power D,we deduce easily the reasonable parameter value of Eq. (6) to fit the measuring results. Firstly, on the basis of the slope of fitting line, the parameters (C, K^{-1}, η_q) relating to the slope can be determined. Then, according to the intercept of the fitting line, the upconversion parameter γ can be easily obtained. Meanwhile, the dependence of the fractional thermal load η_h on the boundary temperature can be also calculated.

The nonradiative decay time τ_{nr} is only related to doping concentration of the crystal. The fluorescence lifetime τ is measured to be 87 μs for 0.8% doped crystal used in our experiment. On the basis of the expression of the fluorescence lifetime ($1/\tau = 1/\tau_{sp} + 1/\tau_{nr}$, τ_{sp} is the spontaneous lifetime), we obtain easily that the nonradiative decay time τ_{nr} is 669 μs.

The population inversion density Δn above threshold does only depend on the laser loss. For end-pumped lasers with Gaussian pump beam profile, the laser loss increases significantly with the increase of the absorption pump power due to the aberrated nature of thermal lens, which results in an increase of the diffraction loss [25, 26]. As a result, the population inversion density Δn is not held constant with the change of the pump power. However, the current laser pumped by a fiber-coupled laser diode with 'Top-hat' beam profile, the thermal lens has no high-order phase aberration within the pumped region. We do always choose $\omega_L < \omega_p$ to eliminate the high-order aberration and the diffraction loss during the measuring process [27]. At the same time, in order to minimize the influence of the variation of the pump power on the diffraction loss, the measurement results of the dioptric power are limited to the range of 6.3 m^{-1} to 8 m^{-1}. The radius of the corresponding laser mode, at the position of the laser crystal, is only in the range of 416 μm to 426 μm, which is less than that of the pump mode. Thus, the dependence of the population inversion density Δn (relative to the diffraction loss) on the dioptric power can be neglected, the population inversion density Δn is considered as a constant within this range.

According to the nonradiative decay time τ_{nr}, the population inversion density Δn, and the intercept of the fitting line, the upconversion parameter γ can be easily obtained at every boundary temperature. According to the measuring results, the dependence of the fractional thermal load η_h on the boundary temperature can be also calculated.

#191256 - $15.00 USD Received 28 May 2013; revised 12 Jul 2013; accepted 12 Jul 2013; published 19 Jul 2013

3. Experimental results and analysis

3.1. Upconversion parameter and fractional thermal load

With the model above, we consider the upconversion-induced heat generation in Nd:YVO_4 crystals, which is end-pumped by a fiber-coupled laser diode at different boundary temperatures, and establish the relation between the dioptric power and the absorbed pump power based on the measuring results. The Nd:YVO_4 crystal is wrapped with indium foil and mounted into a copper housing, whose temperature is controlled by a thermoelectric cooler. A thermistor is embedded in the copper housing to measure the boundary temperature of the laser crystal. A figure "8" ring cavity is adopted to obtain the dioptric power by measuring the parameter of the output beam [28, 29]. Subsequently, we calculate the dioptric power in the boundary temperature range of 293 K to 353 K based on the measuring results of the parameter of the laser output beam. Further reducing the boundary temperature to 283 K, the end-faces of the Nd:YVO_4 will be covered with steam since they are exposed to air. Ultimately, the Nd:YVO_4 fracture will occur.

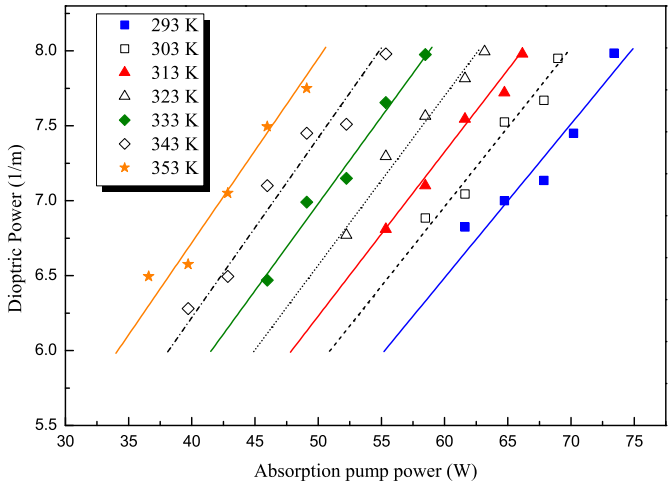

Fig. 1. Dioptric power versus absorbed pump power at 7 different boundary temperatures ranging from 293 K to 353 K. Dots are measuring results of the dioptric power and the lines are the theoretical fitting.

Figure 1 shows the experimental data and theoretical fitting of the dioptric power at different boundary temperatures of Nd:YVO_4. The experimental results show that the dioptric power almost linearly increases with the absorbed pump power between 293K and 353K. We know, on the basis of the analysis of section 2, that the thermo-optical coefficient ds/dT, nonradiative decay time τ_{nr} and population inversion density Δn keep small variation with the change of the temperature and pump power. In the theoretical simulation, the invariable parameters at different boundary temperatures are shown as follows: ds/dT=3.0$\times 10^{-6}$ K^{-1}, τ_{nr}=669 μs, $\Delta n = 0.5 \times 10^{24}$, ω_p=533 μm, η_q=16.5%. The thermal conductivity K_0 at T_0=300 K is 5.23 W/m·K. The values of the upconversion parameter γ, obtained from Eq. (6) and the fitting curves, are 1.4$\times 10^{-21}$ m^3/s, 4.5$\times 10^{-21}$ m^3/s, 6.1$\times 10^{-21}$ m^3/s, 7.8$\times 10^{-21}$ m^3/s, 10.3$\times 10^{-21}$ m^3/s, 12.8$\times$ 10^{-21} m^3/s and 16.5$\times$ 10^{-21} m^3/s, respectively, at the boundary temperatures of 293 K, 303 K, 313 K, 323 K, 333 K, 343 K and 353 K. However, limited by the temperature gradient within the Nd:YVO_4 and the uncertainty of measuring results, the results do only demonstrate the trend of the upconversion parameter γ with temperature, and can not indicate

#191256 - $15.00 USD Received 28 May 2013; revised 12 Jul 2013; accepted 12 Jul 2013; published 19 Jul 2013

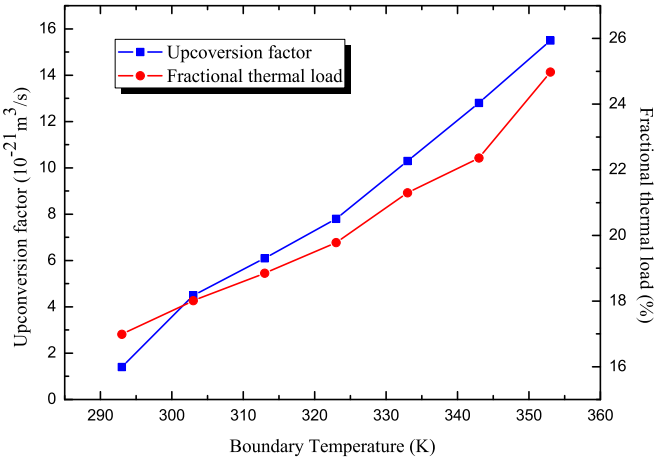

Fig. 2. Upconversion factor γ and fractional thermal load η_h versus boundary temperature of the Nd:YVO_4 crystal.

accurately the γ value at different temperatures. The trends of η_h and γ at different boundary temperatures are shown in Fig. 2. The analysis results show that the fractional thermal load η_h and the upconversion parameter γ increase with the rise of boundary temperature of Nd:YVO_4 crystal. The phenomenon can be explained by the fact that the efficiency of the spectral overlap between laser transition and upconversion transition increases with the rise of boundary temperature. It is due to the thermally induced line broadening mechanism in the absorption (emission) line of acceptor (donor) ion, thermally induced band shifts as well as thermally induced changes in the population of different Nd^{3+} sub-Stack levels [16, 30, 31]. The thermal broadening and shift of the transition line attribute to direct one-phonon process and stationary effects of the phonon-ion interaction [32, 33]. The increase of the upconversion parameter intensifies the nonradiative transitions, as a result, the fractional thermal load η_h increases.

To the best of our knowledge, it is the first time that the dependence of the upconversion factor and the fractional thermal load on boundary temperatures in Nd:YVO_4 is estimated. The probable reasons why there is a deviation between the experimental data points and fitting curves is that the dioptric power depends on several experimental factors and crystal parameters, such as the temperature dependence of the thermal conductivity, thermo-optical coefficient, etc.

3.2. Laser experiments

The scheme of the laser cavity is shown in Fig. 3. Based on the ABCD transfer matrix and the condition of the laser stable mode operation, ($|A+D|<2$) [34], considering the optimal coupling condition of intracavity frequency doubling laser and the minimum thermal effect of the Nd:YVO_4 crystal, the cavity length of the ring cavity is determined. The distance between M_3 and M_4 is fixed at 95 mm and the length of the laser path outside M_3 and M_4 ($M_1 \rightarrow M_2$+$M_2 \rightarrow M_3$+$M_4 \rightarrow M_1$) is kept at 604 mm. The function of the beam radius ω(at the position of the Nd:YVO_4 crystal) versus the thermal lens f_t is shown in Fig. 4. It can be seen that, if the thermal lens f_t fluctuates in a range around 100 mm (about from 88 mm to 262 mm), the laser can still operate in the stable region. Further shortening the length between M_3 and M_4, the stable region of the laser operation moves toward shorter thermal lens f_t. However, it must be said that shorter cavity length makes the stable region of the laser operation narrow, which is adverse to the stability of the laser. Thus, the maximum output power is also limited

#191256 - $15.00 USD Received 28 May 2013; revised 12 Jul 2013; accepted 12 Jul 2013; published 19 Jul 2013

by thermal lens driving the cavity towards the boundary of stable region. At certain laser, the thermal lens (dioptric power) is only dependent of a combination of fractional thermal load η_h and absorption pump power P_{abs}. In order to increase the output power of the laser, the only method we can do is that minimizes the fractional thermal load η_h, to enables higher pump power to inject, while does not increase the thermal load of the gain medium. According to the measuring and analytic results of section 3.1, the lower boundary temperature is benefit of mitigating the fractional thermal load η_h and increasing the output power of the laser.

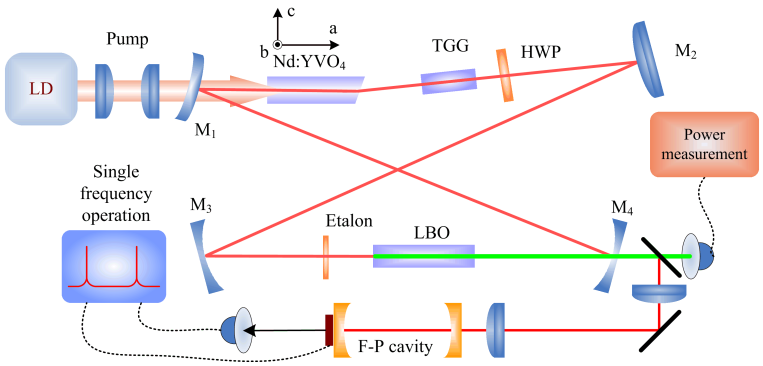

Fig. 3. Experimental setup of the single-frequency green laser. TGG: terbium gallium garnet; HWP: half wave plate; LBO: lithium triborate.

The Nd:YVO_4 crystal has a wedge shape end-facet of 1.5-degree at the exit facet [35], doped concentration of 0.8% and length of 20 mm. A LBO crystal, with the dimensions of $3\times3\times15$ mm^3 and type one non-critical phase matching, is used as the nonlinear crystal for intracavity frequency-doubling. To maintain the unidirectional operation of the laser, an optical diode consisting of a 10 mm-long terbium gallium garnet (TGG) rod and an AR-coated zeroth-order half-wave plate (HWP) at 1064 nm is applied. A magnetic field of 0.6 T is forced on the TGG rod to provide about 6-degree polarization rotation for the fundamental wave. An etalon is inserted into the laser resonator as a spectral filter to narrow the gain bandwidth and ensure the stability of the single-frequency operation.

During the process of increasing pump power, the thermal load of the laser crystal increases gradually, the f_t shortens gradually. Until the f_t is less than 262 mm (from Fig. 4), the laser satisfies the condition of the stable mode operation and starts to oscillate. When the boundary temperature of the Nd:YVO_4 crystal is controlled at 7 different temperatures ranging from 293 K to 353 K, the output power vs. the absorption pump power is shown in Fig. 5. The pumping threshold at the boundary temperature of 293 K is about 21.1 W, while it is 17.9 W at 353 K, which is lower than that of 293 K. This can be explained by the larger η_h at 353 K, in which a lower power level is enough to make $f_t<262$ mm, the laser starts to oscillate.

After the pump power exceeds the threshold, the output power increases monotonously with pump-power until it reaches the maximum value. However, owing to the discrepancy of η_h, the laser shows different output power characteristic curves for these cases of different boundary temperatures. This phenomenon can be explained by the conclusion that the fractional thermal load η_h increases with the rise of boundary temperature with lasing. At the boundary temperature of 293 K, the lowest temperature in our experiment, the fractional thermal load η_h is lower, which permits higher pump power to inject meanwhile keeps the cavity in the stable region. 25.3 W of output power of single-frequency green laser is obtained at the absorption pump power of 78.5 W. However, for the boundary temperature of 353 K, due to the larger fractional thermal load η_h, a lower pump power can induce enough dioptric power D and make the laser

#191256 - $15.00 USD Received 28 May 2013; revised 12 Jul 2013; accepted 12 Jul 2013; published 19 Jul 2013

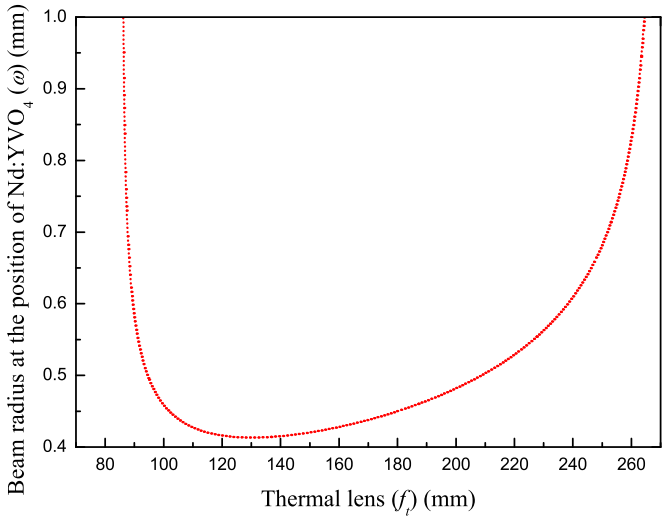

Fig. 4. Beam radius of fundamental wave in Nd:YVO_4 as a function of thermal focal length of the Nd:YVO_4 crystal.

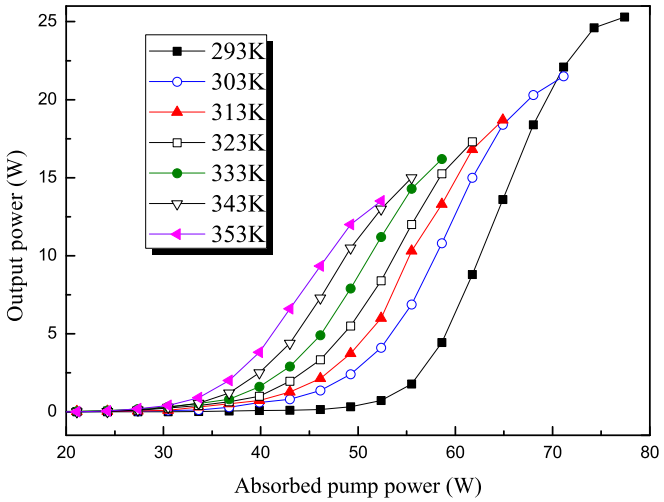

Fig. 5. Laser output power vs absorption pump power at 7 different boundary temperatures ranging from 293 K to 353 K.

out of the stable region. Only 53 W of the absorbed pump power can be injected, corresponding to a maximum output power of 13 W. The similar analysis is omitted at other temperatures. According to Fig.1 and Fig. 5, we know that all the maximum output powers at different boundary temperature are obtained under the condition of the same dioptric power. At this point, the mode radius in the nonlinear crystal is the same, which corresponds to the same conversion efficiency of the intracavity second harmonic generation. So the dependence of the harmonic output power on the boundary temperature can fully represent that of the fundamental wave.

Figure 6 shows the functions of the maximum output power and conversion efficiency versus the boundary temperature of the Nd:YVO_4 crystal. The maximum conversion efficiency

#191256 - $15.00 USD Received 28 May 2013; revised 12 Jul 2013; accepted 12 Jul 2013; published 19 Jul 2013

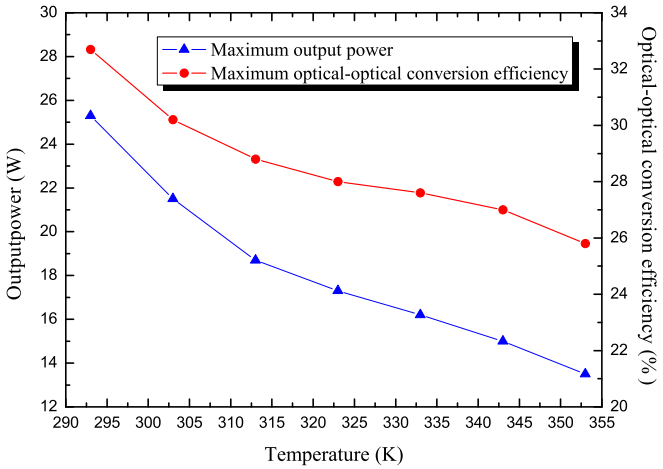

Fig. 6. The dependence of the maximum output power and optical-optical conversion efficiency upon the boundary temperature of the Nd:YVO_4 crystal.

decreases with the rise of boundary temperature, which results from the decrease of SECS (stimulated emission cross section) [17-19] and the increase of ETU process [6]. Reduction in the maximum output power is a superposition result of the decrease of the conversion efficiency and maximum absorbed pump power. The maximum absorbed pump power is limited by the fractional thermal load η_h, which is in close approximation of quantum defect with the reduction of boundary temperature. On the basis of the above analysis, we believe that further power scaling can come true by reducing the Nd:YVO_4 temperature to less than 293 K.

4. Conclusion

In summary, we have analyzed the thermal effect of Nd:YVO_4 crystal operating at different boundary temperatures by measuring the dioptric power. In combination of the theoretical analysis with measuring results of the dioptric power, we obtain the fractional thermal load η_h and the upconversion parameter γ at different boundary temperatures. In the analysis process, since these parameters (dn/dT, Δn) have a very small temperature coefficient, its influence on the dioptric power can be neglected. We consider mainly the temperature-dependent thermal conductivity K and obtain the dependence of the upconversion parameter γ on the boundary temperature. Measurement and analysis results show that the values of η_h and γ present a considerable increase with the increasing of boundary temperature under the condition of lasing. The increase of γ is explained by the fact that the efficiency of the spectral overlap between laser transition and upconversion transition increases with temperature. As a result, the nonradiative transition enhances gradually, which makes η_h get into a higher level.

Subsequently, we construct the experimental setup of high-power single-frequency laser and measure the output characteristic of the laser at different boundary temperatures. Experimental results show that the maximum output power and conversion efficiency of the laser decreases obviously with the rise of boundary temperature, which is attributed to low SECS and high upconversion parameter. In addition, the increasing η_h with the rise of temperature limits the maximum pump power injecting, which is another reason that the maximum output power decreases.

Therefore, designing a high power Nd:YVO_4 laser system does not only involve managing thermal lens resulted from the temperature gradient, but also involves working with laser crys-

#191256 - $15.00 USD Received 28 May 2013; revised 12 Jul 2013; accepted 12 Jul 2013; published 19 Jul 2013

tals having lower performance due to the absolute boundary temperature increase. Base on the experimental and theoretical analysis results, it is certainly possible to scale the output power to higher by controlling effectively the Nd:YVO_4 temperature to a lower.

Acknowledgments

This research is supported by the National Basic Research Program of China (2010CB923101), the National Nature Science Foundation of China (61008001) and the Nature Science Foundation of Shanxi Province (2011021003-2).

#191256 - $15.00 USD Received 28 May 2013; revised 12 Jul 2013; accepted 12 Jul 2013; published 19 Jul 2013